Theoretical study of the visible and ultraviolet spectra of chromyl chloride (CrO_2Cl_2)

Koji Yasuda and Hiroshi Nakatsuji
Department of Synthetic Chemistry, Faculty of Engineering, Kyoto University, Kyoto 606, Japan
and Institute for Fundamental Chemistry, 34-4, Takano-Nishihikari-cho, Sakyo-ku, Kyoto 606, Japan

(Received 22 February 1993; accepted 19 April 1993)

The excitation spectrum of chromyl chloride (CrO_2Cl_2) is studied theoretically by the symmetry adapted cluster-configuration interaction (SAC-CI) method. The calculated spectrum agrees well with the observed spectrum. In this report, we describe the assignments of the visible and ultraviolet spectra up to 8.0 eV and discuss the nature of the excitations.

I. INTRODUCTION

Since the first report by Étard in 1881,[1] chromyl chloride (CrO_2Cl_2) has been the subject of a number of investigations. Of particular interest has been its strong and specific ability to oxidize various organic compounds, i.e., the Étard reaction. About a decade ago, Rappé and Goddard reported on the epoxidation and olefin metathesis reactions of group IV oxo transition metal species.[2] Chromyl chloride is one of the few transition metal complexes which have a relatively high vapor pressure. Because of its deep color and high vapor pressure, the spectrum of chromyl chloride has been the subject of several experimental investigations since 1926.[3–11] Various experimental studies have recently revealed the nature of the lowest excited states.[5–10]

On the other hand, only a few theoretical studies have examined the electronic structures of the relatively low excited states.[4,12] Figure 1 summarizes the *ab initio* calculations for the excitation energies of CrO_2Cl_2. Thus far, there has been no theoretical study of the entire visible and ultraviolet (VUV) spectra. Jasinski and co-workers have measured gas phase electronic absorption spectra of CrO_2F_2 and CrO_2Cl_2 in the visible and near ultraviolet regions.[4] They explained these spectra using molecular orbital calculations based on the self-consistent field (SCF)-$X\alpha$-SW method, and correlated the results with those for the isoelectronic species CrO_4^{2-} and MnO_4^-. They also explained fine vibrational progressions which they observed in the absorption spectra. However, based on their calculations, the lowest excited state has a B_1 symmetry, which does not agree with the results of another study.[7] Furthermore, they did not calculate theoretical intensities, which makes it difficult to explain the spectra of low symmetry molecules with many dipole-allowed transitions. Later, Miller and co-workers studied the lower excited states of CrO_4^{2-}, CrO_3X^-, and CrO_2X_2, with X=F and Cl, using the SCF-$X\alpha$-SW method.[12] They successfully reproduced both the energy and symmetry of the lowest excited state of CrO_2Cl_2, but their result was limited to the energy region below 3.5 eV.

In this study, we investigate the excited states of CrO_2Cl_2 in order to explain the VUV spectrum up to 8.0 eV, and to determine the electronic nature of the excited states. We use the symmetry adapted cluster (SAC)[13]/symmetry adapted cluster-configuration interaction (SAC-CI)[14] method, which has been applied to several transition metal complexes.[15–20] This method has been shown to be useful for investigating excited states over a wide energy range and has yielded many reliable assignments in experimental spectra.

II. COMPUTATIONAL DETAILS

CrO_2Cl_2 possesses C_{2v} symmetry. Its atomic coordinates, as determined by electron diffraction,[21] are shown in Table I.

Since the effective core potential (ECP) yields rather poor results for excited states,[19] we used all-electron basis sets as follows. For the Cr atom, we used Huzinaga's $(14s8p5d)/[6s2p2d]$ set together with two *p*-type polarization functions ($\zeta_p=0.109$, 0.036).[22] For the Cl and O atoms, we used Huzinaga's $(11s8p)/[5s3p]$ set and the $(9s5p)/[4s2p]$ set, respectively.[22,23] Since we were interested only in the valence excitations, we did not use the Rydberg basis functions.

The electron correlations in the ground state were calculated by the SAC method.[13] The Hartree–Fock (HF) molecular orbitals (MOs) were used as reference orbitals. The excited states were calculated by the SAC-CI method.[14] The calculation was performed using the SAC85 program.[24] The active space in the SAC/SAC-CI calculation consisted of 16 occupied orbitals and 36 unoccupied orbitals. All single-excitation operators were included without selection. The double-excitation operators in the linked term were selected by the second-order perturbation method.[25] For the ground state, double-excitation operators whose perturbation energies with the HF configuration are larger than 4×10^{-5} a.u. were included. For the singlet and triplet excited states, the thresholds were 4×10^{-5} and 1×10^{-4} a.u., respectively, for the main reference configurations of the excited states. In the SAC/SAC-CI theories, triple and quadruple excitations are included in the unlinked terms as the products of the lower excitation operators. The selections were made as described previously.[25] Table II shows the dimensions of the present calculation.

III. RESULTS

Chromyl chloride (CrO_2Cl_2) has an approximately tetrahedral configuration. Therefore, some similarity be-

0021-9606/93/99(3)/1945/7/$6.00

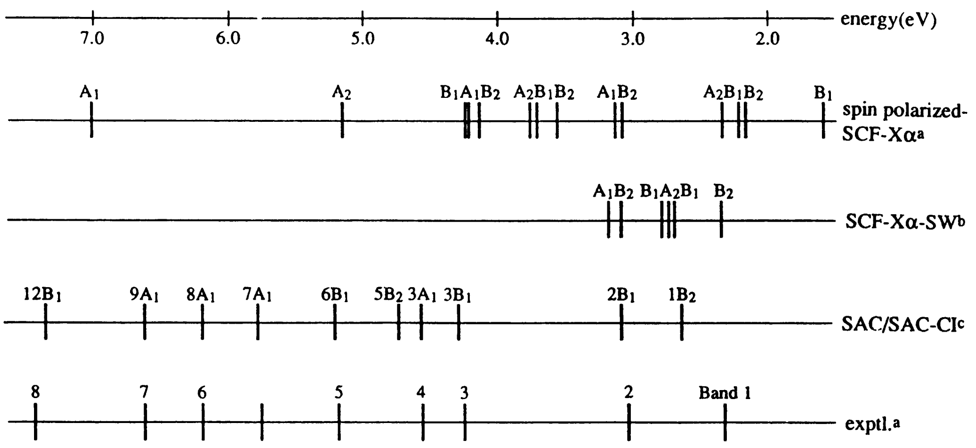

FIG. 1. Summary of the *ab initio* calculations for the excitation energies of CrO_2Cl_2. (a) Jasinski *et al.* (Ref. 4). (b) Miller, Tinti, and Case (Ref. 12). (c) Present calculation.

tween the results of the present calculation and those for tetrahedral molecules such as CrO_4^{2-} (Ref. 20) and MnO_4^- (Ref. 18) might be expected. However, we found it difficult to correspond the MOs and the excited states of these molecules because the decrease in symmetry causes considerable mixing of the orbitals and excited states, as will be seen later.

A. Ground state

The HF orbital energies and the orbital natures of CrO_2Cl_2 in the ground state are shown in Table III, in which σ and π denote local bonding modes and + and − signs show bonding and antibonding combinations, respectively. The five lowest occupied valence MOs are bonding MOs between Cr and O atoms which involve primarily Cr(d) and O(p) orbitals. The three lowest MOs, $13a_1$, $6b_2$, and $8b_1$, roughly correlate to the threefold degenerate t_2 orbitals in the Td symmetry, and the remaining two MOs, $2a_2$ and $14a_1$, correspond to the e orbitals. However this is only a crude approximation. According to the crystal field theory, if the $13a_1$ orbital corresponds to t_2, then this MO should primarily use the Cr(d_{xy}) atomic orbital (AO). However, based on our calculations, two orbitals, $13a_1$ and $14a_1$, use both d_{xy} and d_z^2 to the same extent; a strong mixing occurs between these orbitals.

The $7b_2$ MO is a nonbonding lone-pair orbital localized on the O atoms. Mülliken population analysis shows that about 1.6 electrons are in the O(p) orbitals.

The $15a_1$ MO is a σ-Cr(s)+Cl(p) weakly bonding MO, while the $9b_1$ MO is a Cl(p) nonbonding and π-Cr(p) −O(p) weakly antibonding MO. The Cr($4s$) orbital is used in $15a_1$ and the Cr($4p$) orbital is used in $9b_1$. The $15a_1$ MO corresponds to the a_1 orbital in T_d symmetry.

The four highest occupied MOs are nonbonding lone-pair orbitals localized on the Cl atoms. The $7b_2$, $9b_1$, and $16a_1$ MOs correspond to the t_2 orbitals in T_d symmetry, and the three highest occupied orbitals, $8b_2$, $3a_2$, and $10b_1$, correspond to the t_1 orbitals.

The five lowest unoccupied orbitals are antibonding MOs between Cr and ligands. They have negative orbital energies. The two lower MOs are antibonding between Cr and O and between Cr and Cl, while the other MOs are mainly antibonding between Cr and O.

The HF energy of CrO_2Cl_2 is −2111.191 937 a.u. and the correlation energy calculated by the SAC method is −0.542 259 a.u. The excitations which are important in representing the correlations in the SAC ground state are those from the bonding MOs to the antibonding MOs. Electron correlations are generally very important in transition metal complexes which have many low-energy valence unoccupied MOs.

TABLE I. Atomic coordinates in CrO_2Cl_2 (in atomic units).

Atom	x	y	z
Cr	0	0	0
Cl_1	3.3457	0	−2.2033
Cl_2	−3.3457	0	−2.2033
O_1	0	2.3552	1.8040
O_2	0	−2.3552	1.8040

TABLE II. Dimensions of the SAC/SAC-CI calculation for CrO_2Cl_2.

State	Symmetry	Dimension	Threshold
Ground	$^1A_1$	3566	4.0×10^{-5}
Excited	$^1A_1$	6828	4.0×10^{-5}
	$^1A_2$	6601	
	$^1B_1$	6711	
	$^1B_2$	6530	
	$^3A_1$	7271	1.0×10^{-4}
	$^3B_1$	7234	
	$^3B_2$	7322	

B. Excited states

Table IV summarizes the excitation energies, oscillator strengths, and main configurations of the singlet excited

TABLE III. Orbital energy and orbital nature of CrO_2Cl_2.

MO	Symmetry	Orbital energy (a.u.)	Orbital nature[a]	
Valence occupied MO				
26	$13a_1$	−0.705 41	σ,π-Cr(d)+O(p)	
27	$6b_2$	−0.700 18	σ-Cr(d)+O(p)	
28	$8b_1$	−0.646 46	π-Cr(d)+O(p)	σ-Cr(d)+Cl(p) (weakly)
29	$2a_2$	−0.645 95	π-Cr(d)+O(p)	
30	$14a_1$	−0.631 82	σ-Cr(d)+O(p)	
31	$7b_2$	−0.581 18	O(p)	
32	$15a_1$	−0.568 37	σ-Cr(s)+Cl(p)	
33	$9b_1$	−0.545 48	Cl(p)	π-Cr(p)−O(p)
34	$16a_1$	−0.536 77	Cl(p)	
35	$8b_2$	−0.512 58	Cl(p)	
36	$3a_2$	−0.492 73	Cl(p)	
37	$10b_1$	−0.485 96	Cl(p)	
Low-lying unoccupied MO				
38	$11b_1$	−0.083 70	π-Cr(d)−O(p)	σ-Cr(d)−Cl(p)
39	$17a_1$	−0.075 13	σ-Cr(d)−O(p)	
40	$4a_2$	−0.073 29	π-Cr(d)−O(p)	
41	$18a_1$	−0.021 94	σ-Cr(d)−O(p)	
42	$9b_2$	−0.009 74	σ-Cr(d)−O(p)	

[a] + and − signs indicate bonding and antibonding combinations, respectively.

states. The excitation energies of the low-lying triplet states are shown in Table V. The generally accepted assignment for the lowest excited state of tetrahedral closed-shell transition metal complexes is the charge transfer state from ligand to metal (LMCT), $t_1 \rightarrow e$, which leads to the T_1 or T_2 state. There is also a general agreement that the dipole-forbidden T_1 state lies below the dipole-allowed T_2 state.[12] The present result for CrO_2Cl_2 agrees with this model if the three lowest excited states, $1B_2$, $1B_1$, and $1A_2$, correspond to the T_1 state, and the $2B_1$, $1A_1$, and $2B_2$ states correspond to the T_2 state. For higher energy regions, it is difficult to make a clear correspondence between our findings and those for tetrahedral molecules.

Lower energy excited states below ~5 eV are characterized as transitions from the nonbonding ligand MOs to the antibonding Cr-ligand MOs. Higher energy excited states above ~7 eV are characterized as transitions from the bonding Cr+ligand MO to the antibonding Cr-ligand MO. A strong mixing between these two types of transitions occurs in the medium energy region of ~6 eV and makes the spectrum rather complicated.

The single excitation CI (SECI) method does not provide accurate excitation energies. For example, the lowest singlet excited state, as calculated by the SECI method, is $1A_2$ with an excitation energy of 3.09 eV, which does not agree with experiments in both symmetry and excitation energy.[4,7] Similar discrepancies can also be seen for higher excited states. Therefore, electron correlations are very important for adequate descriptions of the excited states of this molecule. This is generally true for the excited states of metal complexes.[17–20]

C. Nature of the excited states

The room-temperature, gas phase electronic absorption spectrum of CrO_2Cl_2 is shown in Figs. 2 (2–6 eV) and 4 (5.5–8 eV). The spectrum consists of eight separate areas of absorption,[4] which are referred to as bands 1–8, as follows: (1) a weak absorption band with many associated fine structures from 2.0 to 2.6 eV; (2) an intense, broad, featureless band from 2.6 to 3.5 eV; (3) a very intense band with vibrational structures from 3.8 to 4.3 eV; (4) a highly structured band from 4.3 to 4.9 eV with less intensity than band 3 and appearing as a shoulder on the higher energy side of that band; (5) an intense band from 5.0 to 5.7 eV with a single, regular vibrational progression; (6) a featureless band at 6.2 eV appearing as a shoulder of band 7; (7) an intense, broad, featureless band centered at 6.6 eV; and (8) an intense, broad, featureless band centered at 7.4 eV.

Band 1 can be assigned using various experimental results and the present calculation. First, rotational analysis has shown that the lowest excited singlet state is $^1B_2$ in our coordinate system.[7] Second, in the crystalline spectrum of CrO_2Cl_2, the first absorption band centered at 2.3 eV consists of two systems of peaks.[8] System 2 at 2.33 eV lies in a higher energy region than system 1 at 2.30 eV, and is at least 16 times more intense than system 1. The vibrational progression frequency in system 1 is lower than that for system 2, but their vibrational pattern is exactly the same. These findings suggest that system 1 is the triplet analog of system 2.[8,9]

Based on our calculation, the $1\,^1B_2$ and $1\,^3B_2$ states are within this region, and the $^1B_1$ and dipole-forbidden $^1A_2$ states are at ~2.9–3.0 eV (see Fig. 3, Tables IV and V). This suggests that system 1 at 2.30 eV, which has a weaker intensity, can be attributed to the $1\,^3B_2$ state calculated at 2.42 eV, and that system 2 at 2.33 eV can be attributed to the $1\,^1B_2$ state calculated at 2.63 eV. The lowest singlet–triplet separation has been estimated to be <0.03 eV in various solid hosts,[8,9] while the calculated separation en-

TABLE IV. Excitation energies and oscillator strengths for the singlet excited states of CrO_2Cl_2.

Excitation energy						
Expt.[a]	Calc.	State	Oscillator strength	Main configurations (coefficients)[b]		
2.33	2.63	$1B_2$	7.62×10^{-3}	$8b_2\rightarrow17a_1\ (-0.65)$	$7b_2\rightarrow17a_1\ (-0.63)$	
	2.88	$1B_1$	8.50×10^{-4}	$7b_2\rightarrow4a_2\ (0.71)$	$8b_2\rightarrow4a_2\ (0.52)$	
	3.00	$1A_2$	forbidden	$3a_2\rightarrow17a_1\ (-0.92)$		
3.04	3.10	$2B_1$	4.70×10^{-2}	$10b_1\rightarrow17a_1\ (0.79)$		
	3.41	$2A_2$	forbidden	$8b_2\rightarrow11b_1\ (0.66)$	$7b_2\rightarrow11b_1\ (0.66)$	
	3.71	$1A_1$	2.39×10^{-3}	$16a_1\rightarrow17a_1\ (-0.63)$	$10b_1\rightarrow11b_1\ (-0.51)$	
	3.97	$2B_2$	1.31×10^{-3}	$8b_2\rightarrow17a_1\ (0.64)$	$7b_2\rightarrow17a_1\ (-0.53)$	
	4.08	$3B_2$	1.40×10^{-3}	$3a_2\rightarrow11b_1\ (-0.68)$	$10b_1\rightarrow4a_2\ (-0.47)$	
	4.10	$2A_1$	5.05×10^{-3}	$10b_1\rightarrow11b_1\ (-0.74)$	$3a_2\rightarrow4a_2\ (0.49)$	
	4.12	$4B_2$	5.10×10^{-4}	$3a_2\rightarrow11b_1\ (0.60)$	$10b_1\rightarrow4a_2\ (-0.60)$	
4.24	4.28	$3B_1$	3.90×10^{-2}	$9b_1\rightarrow17a_1\ (-0.80)$		
	4.39	$3A_2$	forbidden	$16a_1\rightarrow4a_2\ (0.64)$	$14a_1\rightarrow4a_2\ (0.55)$	
	4.54	$3A_1$	2.72×10^{-2}	$3a_2\rightarrow4a_2\ (0.74)$		
4.56	4.63	$4B_1$	1.62×10^{-4}	$16a_1\rightarrow11b_1\ (0.73)$		
	4.736	$5B_2$	1.92×10^{-2}	$8b_2\rightarrow18a_1\ (0.54)$	$10b_1\rightarrow4a_2\ (0.47)$	$7b_2\rightarrow18a_1\ (0.45)$
	4.787	$4A_1$	5.27×10^{-3}	$15a_1\rightarrow17a_1\ (0.79)$		
	4.84	$4A_2$	forbidden	$3a_2\rightarrow18a_1\ (-0.55)$	$8b_2\rightarrow11b_1\ (-0.52)$	$7b_2\rightarrow11b_1\ (0.49)$
	4.97	$5B_1$	3.94×10^{-3}	$10b_1\rightarrow18a_1\ (0.62)$		
	5.15	$5A_1$	1.84×10^{-5}	$7b_2\rightarrow9b_2\ (0.66)$	$8b_2\rightarrow9b_2\ (0.51)$	
5.22	5.22	$6B_1$	1.13×10^{-2}	$8b_2\rightarrow4a_2\ (0.59)$		
	5.35	$5A_2$	forbidden	$3a_2\rightarrow18a_1\ (0.69)$	$8b_2\rightarrow11b_1\ (-0.44)$	
	5.38	$7B_1$	3.87×10^{-3}	$8b_1\rightarrow17a_1\ (-0.76)$	$10b_1\rightarrow18a_1\ (-0.47)$	
	5.40	$6B_2$	6.12×10^{-3}	$9b_1\rightarrow4a_2\ (-0.80)$		
	5.47	$6A_1$	2.67×10^{-5}	$14a_1\rightarrow17a_1\ (-0.53)$	$14a_1\rightarrow18a_1\ (0.44)$	$9b_1\rightarrow11b_1\ (0.42)$
	5.75	$6A_2$	forbidden	$2a_2\rightarrow17a_1\ (-0.66)$	$10b_1\rightarrow9b_2\ (-0.47)$	
5.77	5.78	$7A_1$	3.21×10^{-2}	$9b_1\rightarrow11b_1\ (-0.47)$	$14a_1\rightarrow17a_1\ (-0.42)$	$16a_1\rightarrow18a_1\ (-0.39)$
	5.91	$7B_2$	6.42×10^{-3}	$6b_2\rightarrow17a_1\ (0.65)$	$6b_2\rightarrow18a_1\ (-0.43)$	
	5.94	$7A_2$	forbidden	$15a_1\rightarrow4a_2\ (0.57)$	$16a_1\rightarrow4a_2\ (0.50)$	
	6.01	$8B_1$	3.01×10^{-2}	$14a_1\rightarrow11b_1\ (-0.65)$	$9b_1\rightarrow18a_1\ (-0.40)$	
	6.19	$9B_1$	2.19×10^{-2}	$3a_2\rightarrow9b_2\ (-0.79)$		
6.20	6.19	$8A_1$	1.02×10^{-1}	$16a_1\rightarrow18a_1\ (-0.56)$	$9b_1\rightarrow11b_1\ (0.45)$	
	6.23	$8A_2$	forbidden	$15a_1\rightarrow4a_2\ (-0.55)$	$10b_2\rightarrow9b_2\ (-0.48)$	
	6.27	$9A_2$	forbidden	$10b_1\rightarrow9b_2\ (0.59)$	$14a_1\rightarrow4a_2\ (-0.48)$	
	6.45	$8B_2$	5.07×10^{-3}	$8b_2\rightarrow18a_1\ (-0.56)$	$7b_2\rightarrow18a_1\ (0.49)$	$8b_1\rightarrow4a_2\ (-0.46)$
6.63	6.51	$9A_1$	3.28×10^{-2}	$13a_1\rightarrow17a_1\ (-0.79)$		
	6.53	$10B_1$	5.90×10^{-3}	$9b_1\rightarrow18a_1\ (-0.63)$	$15a_1\rightarrow11b_1\ (0.42)$	$14a_1\rightarrow11b_1\ (0.42)$
	6.81	$9B_2$	9.46×10^{-5}	$8b_1\rightarrow4a_2\ (-0.58)$	$16a_1\rightarrow9b_2\ (-0.39)$	
	6.95	$10A_2$	forbidden	$13a_1\rightarrow4a_2\ (0.89)$		
	6.99	$10A_1$	2.99×10^{-3}	$2a_2\rightarrow4a_2\ (-0.71)$		
	7.00	$10B_2$	2.08×10^{-3}	$2a_2\rightarrow11b_1\ (-0.85)$		
	7.19	$11B_1$	3.97×10^{-2}	$6b_2\rightarrow4a_2\ (-0.73)$	$13a_1\rightarrow11b_1\ (-0.39)$	
	7.32	$11A_1$	1.47×10^{-2}	$15a_1\rightarrow18a_1\ (-0.55)$	$8b_2\rightarrow9b_2\ (-0.48)$	$7b_2\rightarrow9b_2\ (0.47)$
7.44	7.33	$12B_1$	8.99×10^{-1}	$15a_1\rightarrow11b_1\ (-0.55)$	$3a_2\rightarrow9b_2\ (0.46)$	
	7.37	$11A_2$	forbidden	$9b_1\rightarrow9b_2\ (0.82)$		
	7.59	$12A_2$	forbidden	$6b_2\rightarrow11b_1\ (0.67)$		
	7.66	$12A_1$	2.87×10^{-2}	$14a_1\rightarrow18a_1\ (-0.62)$	$8b_1\rightarrow11b_1\ (-0.42)$	
	7.70	$13B_1$	3.06×10^{-2}	$13a_1\rightarrow11b_1\ (-0.77)$	$8b_1\rightarrow18a_1\ (-0.43)$	
	7.85	$11B_2$	1.78×10^{-2}	$16a_1\rightarrow9b_2\ (-0.77)$		
	7.97	$13A_2$	forbidden	$2a_2\rightarrow18a_1\ (0.70)$	$6b_2\rightarrow11b_1\ (-0.56)$	

[a] The value shows the center of the observed peak or the center of the vibrational progression.

[b] Only configurations with coefficients larger than 0.39 are shown.

ergy (0.20 eV) is greater by an order of magnitude. However, the former value represents the difference between adiabatic transition energies, rather than between vertical transition energies, and therefore may be expected to be smaller than the calculated separation energies. Miller *et al.* attributed band 1 to the $8b_2\rightarrow17a_1$ transition based on the $X\alpha$-calculation.[12] Our calculation shows that the $1\,{}^1B_2$ state is a superposition of the $8b_2\rightarrow17a_1$ and $7b_2\rightarrow17a_1$ transitions, which are the transitions from the Cl(p) and O(p) nonbonding MOs to the σ-Cr(d)–O(p) antibonding MO, while the $1\,{}^3B_2$ state is a superposition of the $7b_2\rightarrow17a_1$ and $7b_2\rightarrow18a_1$ transitions, which are the charge transfer transitions from the O(p) nonbonding MO to the metal-ligand antibonding MOs. As mentioned above, this $1B_2$ state corresponds to the T_1 state in T_d symmetry, and therefore this assignment agrees with the general aspects of tetrahedral molecules.

There has been some controversy about how many

TABLE V. Excitation energies for the low lying triplet excited states of CrO_2Cl_2.

Excitation energy					
Expt.[a]	Calc.	State	Main configuration (coefficient)[b]		
2.30	2.42	$1B_2$	$7b_2 \rightarrow 17a_1$ (−0.60)	$7b_2 \rightarrow 18a_1$ (0.34)	
	2.64	$1B_1$	$7b_2 \rightarrow 4a_2$ (−0.77)	$8b_2 \rightarrow 4a_2$ (−0.50)	
	2.81	$1A_1$	$3a_2 \rightarrow 4a_2$ (0.56)	$2a_2 \rightarrow 4a_2$ (0.47)	$10b_1 \rightarrow 11b_1$ (0.42)
	2.87	$2B_1$	$10b_1 \rightarrow 17a_1$ (−0.91)		
	3.15	$2B_2$	$3a_2 \rightarrow 11b_1$ (0.56)	$10b_1 \rightarrow 4a_2$ (0.50)	

[a] The value shows the center of the vibrational progression.

[b] Only configurations with coefficients larger than 0.39 are shown.

electronic origins exist for system 2. Dixson and Webster studied the fluorescence spectrum of gaseous CrO_2Cl_2 which had been excited by a dye laser,[6] and reported that system 2 contains an additional electronic state which has an origin ~220 cm^{-1} above the first. On the other hand, Brazy and Levy studied the lifetime of the helium van der Waals complex of CrO_2Cl_2,[10] and concluded that the second electronic state was actually a vibrational progression of the first state. Based on our results, if there is a second electronic state in this region, it would either be the singlet $1B_1$ state, which has a very low oscillator strength, or the triplet $1B_1$ state, which is calculated to have about the same energy as the $1\,^1B_2$ state. However, our calculations place the $1\,^1B_1$ state too far from the $1\,^1B_2$ state, and the $^3B_1$ state does not couple with the $^1B_2$ state by a spin–orbit coupling mechanism. Therefore, we prefer the assignment suggested by Brazy and Levy.

Band 2 has its maximum at 3.0 eV and is attributed to the $2B_1$ state calculated at 3.10 eV. It represents the transition from the Cl(p) nonbonding MO to the σ-Cr(d)–O(p) antibonding MO. Therefore, the metal-ligand bond should be relaxed in the excited state. As mentioned previously, band 2 has no vibrational structure. If a transition results in a repulsive state, the band should be broad and featureless.[26] We did not examine whether or not the $2B_1$ state is dissociative, but our calculation shows that there is no other state in this region which has a reasonable oscillator strength. It is interesting to note that the photochemical quantum yield of CrO_2Cl_2 decomposition rises rapidly from zero at 3.0 eV to approximately one at higher energies.[11] Further study is anticipated regarding the nature of this decomposition reaction.

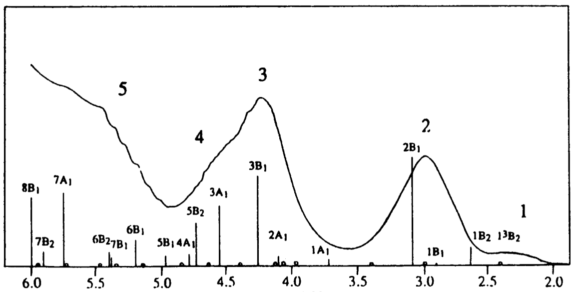

FIG. 2. SAC-CI theoretical excitation spectrum of CrO_2Cl_2 compared with the observed visible spectrum (Ref. 4).

Band 3 has its maximum at 4.2 eV. This band is attributed to the $3B_1$ state, calculated at 4.28 eV, which represents the transition from the Cl(p), π-Cr(p)–O(p) MO to the σ-Cr(d)–O(p) antibonding MO; the former MO has a lone-pair character on the ligands. As shown in Table IV, five other states with small oscillator strengths exist at the lower energy side of this band.

Band 4, centered at 4.5 eV, appears as a shoulder of band 3 and is nonsymmetrical, which suggests that it may have more than one electronic origin. Based on our calculation, we have attributed band 4 to the $3A_1$ and $5B_2$ states, which have reasonable excitation energies and intensities. The $3A_1$ state is the transition from the Cl(p) nonbonding MO to the π-Cr(d)–O(p) antibonding MO, while the $5B_2$ state is the transition from the Cl(p) and O(p) nonbonding MOs to the σ,π-Cr(d)–O(p) antibonding MOs. According to Jasinski and co-workers, only one electronic origin is required to assign a vibrational progression in band 4, and there is no positive evidence for the existence of two electronic origins.[4] Therefore, we interpret our results to indicate that either of the two states may be repulsive and shows no vibrational structure. We believe that this repulsive state, if it exists, may be $5B_2$, because it is more antibonding in nature.

Band 5, an intense band centered at 5.22 eV, appears as a shoulder in the vacuum ultraviolet spectrum (Fig. 2).

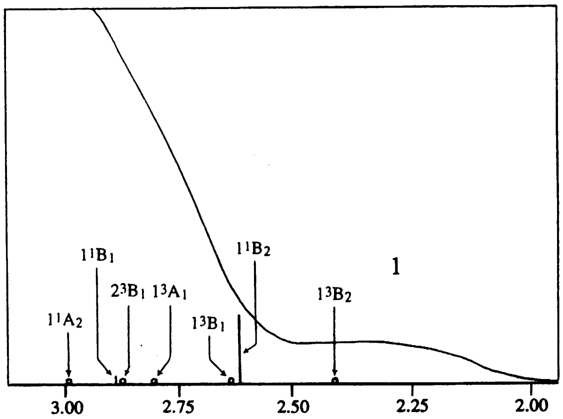

FIG. 3. SAC-CI theoretical excitation spectrum of CrO_2Cl_2 compared with the observed visible spectrum in the region 2.0–3.0 eV (Ref. 4). All singlet and triplet states calculated in this region are shown.

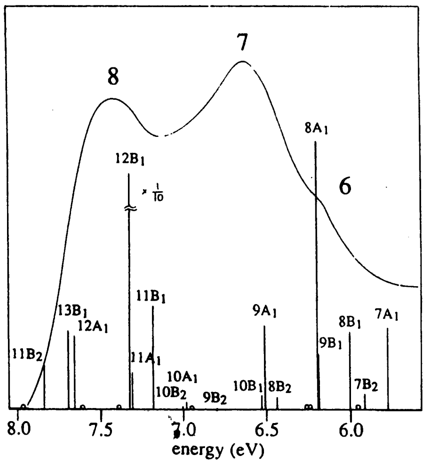

FIG. 4. SAC-CI theoretical excitation spectrum of CrO_2Cl_2 compared with the observed vacuum ultraviolet spectrum (Ref. 4).

Although many states are calculated to be in this region (Table IV), we attribute band 5 to the $6B_1$ state calculated at 5.22 eV, which possesses the largest oscillator strength. Other states, including the $4A_1$ state calculated at 4.79 eV and the $6B_2$ state calculated at 5.40 eV, have about half the oscillator strength of the $6B_1$ state. The $6B_1$ state represents the transition from the Cl(p) nonbonding MO to the π-Cr(d)$-$O(p) antibonding MO. Band 5 also seems to have a shoulder at 5.77 eV in the visible spectrum. This shoulder is attributed to the $7A_1$ state, which is calculated at 5.79 eV. This state is expressed as a linear combination of three main excitations, $9b_1 \rightarrow 11b_1$, $14a_1 \rightarrow 17a_1$, and $16a_1 \rightarrow 18a_1$. As can be seen from the orbital nature shown in Table III, this state has two characters, i.e., charge transfer from ligand to metal and transition from bonding MO to antibonding MO.

Band 6 appears (Fig. 4) as a low energy shoulder at 6.2 eV of band 7 centered at 6.6 eV. There are three dipole-allowed transitions near this shoulder, i.e., $8B_1$ at 6.01 eV, $9B_1$ at 6.19 eV, and $8A_1$ at 6.19 eV. The $8A_1$ state is the primary state of band 6 from the standpoint of both energy and intensity. Therefore, this shoulder is attributed to the $8A_1$ state calculated at 6.19 eV. This state is a superposition of two excitations, $16a_1 \rightarrow 18a_1$ and $9b_1 \rightarrow 11b_1$. These excitations are from nonbonding to antibonding MOs. The $8A_1$ state also incorporates a charge transfer from ligands to metal.

Band 7 is a strong band at 6.6 eV and is attributed to the $9A_1$ state calculated at 6.51 eV. Since the calculated intensity of the $9A_1$ state is smaller than that of the $8A_1$ state, we think that the strong intensity of band 7 is due to the sum of the intensities of the $9A_1$ state and the shoulders of bands 6 and 8. This state is due to the transition from the σ,π-Cr(d)$+$O(p) bonding MO to the σ-Cr(d)$-$O(p) antibonding MO. The strongly repulsive nature of this excited state may explain the fact that this band does not have a vibrational structure. Our calculation also suggest that there are three other states with small oscillator strengths in this region, $8B_2$, $10B_1$, and $9B_2$. The overlap of these states may also explain the lack of a vibrational structure.

Band 8 is a featureless band centered at 7.4 eV and is attributed to the $12B_1$ state calculated at 7.33 eV. Again, our calculation shows that four other states with moderate oscillator strengths exist in this region, $11B_1$, $11A_1$, $12A_1$, and $13B_1$. Nonetheless, the $12B_1$ state is the strongest among them. This state is represented by a linear combination of the two main excitations, $15a_1 \rightarrow 11b_1$ and $3a_2 \rightarrow 9b_2$, which are the transitions from the σ-Cr(s) $+$Cl(p) bonding MO to the π-Cr(d)$-$O(p) and σ-Cr(d)$-$Cl(p)antibonding MO, and from the Cl(p) nonbonding MO to the σ-Cr(d)$-$O(p) antibonding MO. Therefore configuration interaction is very important for a precise description of such a strongly mixed state.

IV. CONCLUSION

We have applied the SAC/SAC-CI method to the calculation of the excited states of CrO_2Cl_2. We have successfully reproduced the VUV spectrum for both excitation energies and intensities in the energy region from 2.4 to 8.0 eV, as shown in Fig. 1. The average discrepancy between the theoretical and experimental values is 0.08 eV. We have provided several new assignments and have described the natures of the excited states. The lower excitations are from the nonbonding ligand MO to the metal-ligand antibonding MO and have charge transfer nature, while the higher excitations are from the metal$+$ligand bonding MO to the metal-ligand antibonding MO. Excitations in the middle energy range are the combinations of these two types of excitations. As compared with the spectra of tetrahedral complexes, CrO_2Cl_2's reduced symmetry causes a considerable mixing of states, which makes its spectrum more complex than those of T_d molecules.

ACKNOWLEDGMENTS

We wish to thank Dr. Hada and Dr. Ehara for their assistance and comments during this study. The SAC/SAC-CI calculations were performed on the FACOM M780 computer at the Data Processing Center of Kyoto University and the HITAC M-680H and S-820 computer at the Institute for Molecular Science. This study was supported in part by a Grant-in-aid for Scientific Research from the Japanese Ministry of Education, Science and Culture.

[1] A. Étard, Ann. Chim. Phys. **22**, 218 (1881).
[2] (a) A. K. Rappé and W. A. Goddard III, J. Am. Chem. Soc. **102**, 5114 (1980); **104**, 448 (1982); (b) Nature **285**, 311 (1980).
[3] (a) A. C. S. Van Heel, Verlag Akad. Wet. Amsterdam **35**, 1112 (1926); Proc. Amst. Acad. **30**, 95 (1927); (b) R. von Ritschl, Z. Phys. **42**, 172 (1927); (c) R. de L. Kronig, A. Schaafsma, and P. K. Peerlkkamp, Z. Phys. Chem. **822**, 323 (1933); (d) P. K. Peerlkamp, Physica **1**, 150 (1933).
[4] J. P. Jasinski, S. L. Holt, J. H. Wood, and L. B. Asprey, J. Chem. Phys. **63**, 757 (1975).
[5] J. R. McDonald, Chem. Phys. **9**, 423 (1975).
[6] R. N. Dixson and C. R. Webster, J. Mol. Spectrosc. **62**, 271 (1976).
[7] J. A. Brazy and D. H. Levy, J. Chem. Phys. **69**, 2901 (1978).
[8] T. M. Dunn and A. H. Francis, J. Mol. Spectrosc. **25**, 86 (1968).

[9] (a) M. Spoliti, J. H. Thirtle, and T. M. Dunn, J. Mol. Spectrosc. **52**, 146 (1974); (b) V. E. Bondybey, Chem. Phys. **18**, 293 (1974); (c) C. L. Lasko, R. M. Miller, and D. S. Tinti, Chem. Phys. Lett. **130**, 359 (1986).

[10] J. A. Brazy and D. H. Levy, Chem. Phys. Lett. **51**, 395 (1977).

[11] R. Halonbrenner, J. R. Huber, U. Wild, and H. Günthard, J. Phys. Chem. **72**, 3929 (1968).

[12] R. M. Miller, D. S. Tinti, and D. A. Case, Inorg. Chem. **28**, 2738 (1989).

[13] H. Nakatsuji and K. Hirao, J. Chem. Phys. **68**, 2053 (1978).

[14] H Nakatsuji, Chem. Phys. Lett. **59**, 362 (1978); **67**, 329, 334 (1979).

[15] H. Nakatsuji, Acta Chim. Hungarica **129**, 719 (1992).

[16] (a) H. Nakatsuji, J. Chem. Phys. **80**, 3703 (1984); (b) H. Nakatsuji, O. Kitao, and T. Yonezawa, *ibid.* **83**, 723 (1985); (c) H. Nakatsuji and O. Kitao, *ibid.* **87**, 1169 (1987); (d) O. Kitao and H. Nakatsuji, Chem. Phys. Lett. **143**, 528 (1988).

[17] (a) H. Nakatsuji and S Saito, J. Chem. Phys. **93**, 1865 (1990); (b) Int. J. Quantum Chem. **39**, 93 (1991); H. Nakatsuji, M. Sugimoto, and S Saito, Inorg. Chem. **29**, 3095 (1990).

[18] H. Nakai, Y. Ohmori, and H. Nakatsuji, J. Chem. Phys. **95**, 8287 (1991).

[19] H. Nakatsuji, M Ehara, M. H. Palmer, and M. Guest, J. Chem. Phys. **97**, 2561 (1992).

[20] H. Nakatsuji, S. Jitsuhiro, and H. Nakai (to be published).

[21] K. J. Palmer, J. Am. Chem. Soc. **60**, 2360 (1938).

[22] S. Huzinaga, J. Andzelm, M. Klobukowski, E. Radzio-Andzelm, Y. Sakai, and H. Tatewaki, *Gaussian Basis Sets for Molecular Calculations* (Elsevier, Amsterdam, 1984).

[23] T. H. Dunning, Jr., J. Chem. Phys. **53**, 2823 (1970).

[24] H. Nakatsuji, Program system for SAC and SAC-CI calculations, Program Library No. 146 (Y4/SAC), Data Processing Center of Kyoto University, 1985; H. Nakatsuji, Program Library SAC85 (No. 1396), Computer Center of the Institute for Molecular Science, Okazaki, 1986.

[25] H. Nakatsuji, Chem. Phys. **75**, 425 (1983).

[26] J. P. Dahl and H. Johansen, Theor. Chim. Acta **8**, 26 (1968).